FFI Norwegian Defence Research Establishment

25/011

FFI-RAPPORT

Application of homogenous scattering theory to an ideally mixed underwater bubble curtain

Martin Fonnum Jakobsen

Application of homogenous scattering theory to an ideally mixed underwater bubble curtain

Martin Fonnum Jakobsen

Norwegian Defence Research Establishment (FFI) 28 February 2025

Keywords
Undervannssprengning
Eksplosiver
Detonasjon
Trykkbølger
Fluidmekanikk
Fluiddynamikk

FFI report
25/011

Project number
1681

Online ISSN
2704-2383

Approvers
Morten Huseby, *Research Manager*
Halvor Ajer, *Director of Research*

The document is electronically approved and therefore has no handwritten signature.

Summary

A bubble curtain is a barrier of rising air bubbles, and it is typically made by driving compressed air through a perforated pipe under water. The bubble curtain can be used as a protective measure to shelter marine life from underwater noise pollution such as controlled underwater explosions, engines, pile driving, and deep-water drilling. In this report we evaluate the protection capabilities of bubble curtains by constructing a simple method to calculate the corresponding sound transmission.

Theoretical considerations predict that the speed of sound in a bubble curtain can be smaller than both the speed of sound in air and water because the presence of the bubbles creates a highly compressible mixture. The effect is primarily dependent on the ratio of the total air volume to the overall volume of the mixture. This key parameter is known as the volume fraction of air.

Due to the small speeds of sound, there is a significant (acoustic) impedance mismatch between the water and bubble curtain. Impedance is a measure of how much a medium resists the flow of internal sound waves and is defined as the product between density and speed of sound. The result of the large impedance mismatch is that the bubble curtain acts as a high-reflective sound shield, under the right conditions. In short, it does indeed hold high protection capabilities.

Our model shows that bubble curtains are most effective in shielding against sound with frequencies up to 100 kHz, although the exact performance varies with certain parameters such as hydrostatic pressure, the size of the bubbles, and the angle of the sound waves relative to the curtain. Our model shows significantly poorer performance of the bubble curtains at frequencies higher than 1 MHz, but the model does not account for disordered localization phenomena in these ranges. An improved future model may shed more light on performance against such frequencies.

Sammendrag

En boblegardin er en barriere av stigende luftbobler. Den lages vanligvis ved å føre komprimert luft gjennom et perforert rør under vann. Boblegardinen kan brukes som et beskyttelsestiltak for å skjerme marint liv fra støyforurensning under vann, for eksempel kontrollerte undervannseksplosjoner, motorer, pæling og dypvannsboring. I denne rapporten evaluerer vi beskyttelsesevnen til boblegardiner ved å konstruere en enkel metode for å beregne den tilsvarende lydtransmisjonen.

Teoretiske betraktninger forutsier at lydhastigheten i en boblegardin kan være mindre enn både lydhastigheten i luft og vann fordi tilstedeværelsen av boblene skaper en svært komprimerbar blanding. Effekten er primært avhengig av forholdet mellom det totale luftvolumet og det totale volumet av blandingen. Denne nøkkelparameteren kalles luftens volumfraksjon.

På grunn av de lave lydhastighetene er det en betydelig forskjell i impedansen mellom vannet og boblegardinen. Akustisk impedans er et mål på hvor mye et medium motstår forplantning av interne lydbølger, og defineres som produktet av tetthet og lydhastighet. Resultatet av den store impedansforskjellen er at boblegardinen fungerer som et høyreflekterende lydskjold, under de rette forholdene. Kort sagt har boblegardinen høy beskyttelsesevne.

Modellen vår viser at boblegardiner er mest effektive i å skjerme mot lyd med frekvenser opp til 100 kHz, selv om den nøyaktige beskyttelsesevnen varierer med visse parametere som hydrostatisk trykk, størrelsen på boblene og vinkelen mellom lydbølgene og boblegardinen. Modellen vår viser betydelig dårligere beskyttelsesevne ved frekvenser høyere enn 1 MHz, men den tar ikke høyde for visse fenomener i disse områdene. En forbedret fremtidig modell kan kaste mer lys over beskyttelsesevnen mot slike frekvenser.

Contents

1 Introduction

There are several contexts in which the Norwegian navy has to perform controlled explosions of sea-mines, torpedos, or other explosive objects. Concretely such contexts usually include: cleaning up remnants of the second world war, testing shock-requirements for the potential purchase of ships or submarines, or training exercises. In any case, these explosions lead to sound waves propagating in the water which can damage (or disturb) marine life or marine infrastructure. To minimize the damage it is important to carefully consider the relevant protective measures.

Sometimes the explosive object can be moved to a distant area away from the unintended targets, so that the sound wave becomes sufficiently damped before it reaches them. In cases where it is hard to evaluate the charge's sensitivity, it is risky to move or approach the charge due to the potential of accidental detonation. In such cases, methods to dampen the sound wave are useful.

One protective measure against the sound wave produced by an underwater explosion are so-called bubble curtains. A bubble curtain is typically made by continuously driving air through one or more submerged perforated pipes. Depending on the amount of air-flow, the resulting wall of bubbles act as a high-impedance barrier capable of blocking sound waves. In 2017 The Norwegian Defence Research Establishment (FFI) performed small-scale experiments that indicated that a bubble curtain can effectively block sound, but the optimal conditions are currently unknown [1].

Predicting the optimal conditions for the damping of a bubble curtain is challenging. The reason is that if the sound frequency matches the bubble resonance frequencies, then the sound wave induces dynamics in the individual bubbles and the bubbles will interact with each other. Taking all of these interactions into account is a complicated matter, even with purely numerical methods such as finite-element analysis and smoothed particle hydrodynamics. An attempt to describe the effects of bubble interactions are exemplified in an elegant and detailed theory constructed by Domenico [2]. The theory takes the following into account: i) heat conduction from the pulsating bubbles, ii) individual bubble sound radiation, and iii) viscous damping by the water on the bubbles.

In this report, we use the scattering theory formalism in combination with the theory of ideal mixtures, to construct a theory which calculates an upper bound for the reflection of sound from a bubble curtain. The scattering theory is simple to use, because the bubbles are treated statically. In the future bubble dynamics can also be incorporated into the theory, but it is not the focus of this report. In its current state the theory predicts optimal reflection conditions that together with Domenico's results paint a clearer picture of how the bubble curtain can be designed with optimal protection capabilities.

2 Bilayer scattering

The theory presented here closely follows [3, 4]. As shown in Fig. 2.1. we consider two adjacent layers labelled medium 1 and 2. Both media are homogenous. In region j (= 1, 2) the density, speed of sound, and impedance are ρ_j, c_j, and $z_j = \rho_j c_j$ respectively. We will consider the scattering

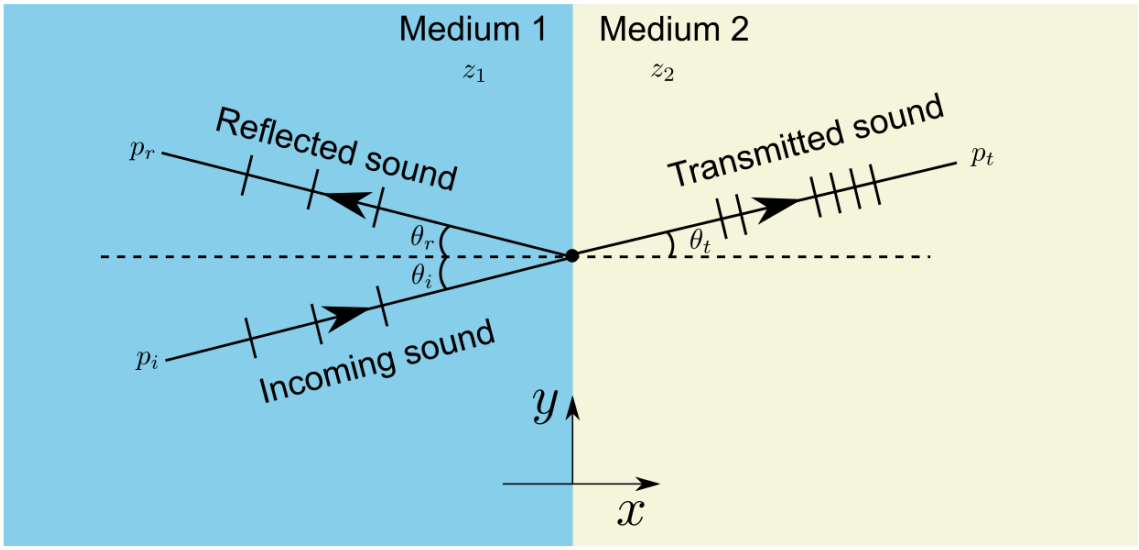

Figure 2.1 An illustration of the sound scattering problem for a bilayer. The incoming sound wave is reflected and refracted at the interface.

problem where a sound wave is incoming from region 1. The solution ansatze for the incoming, reflected, and transmitted waves are

$$\begin{aligned} p_i &= P_i e^{i(\omega t - k_1 x\cos\theta_i - k_1 y \sin\theta_i}, \\ p_r &= P_r e^{i(\omega t + k_1 x\cos\theta_r - k_1 y \sin\theta_r}, \\ p_t &= P_t e^{i(\omega t - k_2 x\cos\theta_t - k_2 y \sin\theta_t}, \end{aligned} \tag{2.1}$$

respectively. The dispersion relation follows by inserting the ansatze into the wave equation and is $k_i = \omega/c_i$. There are two boundary conditions that must be satisifed at the interface $x = 0$:

1. Continuity of pressure: $p_i + p_r = p_t$.
2. Continuity of orthogonal particle velocity: $u_i \cos\theta_i - u_r \cos\theta_r = u_t \cos\theta_t$.

From the pressure boundary condition we obtain Snell's law and its consequences,

$$\begin{aligned} k_1 \sin\theta_i = k_1 \sin\theta_r = k_2 \sin\theta_t, &\qquad \text{(General Snell's law)}, \\ \theta_i = \theta_r, &\qquad \text{(Law of reflection)}, \\ \sin\theta_t = \frac{c_2}{c_1}\sin\theta_i, &\qquad \text{(Law of refraction)}, \\ 1 + R = T, &\qquad \text{(Pressure magnitude matching)} \end{aligned} \tag{2.2}$$

where we in the final line defined the reflection $R = P_r/P_i$ and transmission $T = P_t/P_i$ coefficients. The law of reflection tells us that the angle of incidence is always equal to the angle of reflection,

and the law of refraction reveals that the degree of refraction depends on the sound speed ratio c_2/c_1.

If we use the pressure magnitude matching condition together with the boundary condition on orthogonal particle velocities we obtain explicit expressions for the reflection and transmission coefficients,

$$\begin{aligned} R &= \frac{\frac{z_2}{z_1} - \frac{\cos\theta_t}{\cos\theta_i}}{\frac{z_2}{z_1} + \frac{\cos\theta_t}{\cos\theta_i}}, \\ T &= 1 + R. \end{aligned} \tag{2.3}$$

Using Eq. (2.3) we can also calculate the intensity reflection and transmission coefficients

$$\begin{aligned} R_I &= |R|^2, \\ T_I &= \frac{z_1}{z_2}|T|^2, \\ R_I + T_I &\neq 1. \end{aligned} \tag{2.4}$$

Similarly the power reflection and transmission coefficients are

$$\begin{aligned} R_\Pi &= R_I = |R|^2, \\ T_\Pi &= \frac{\cos\theta_t}{\cos\theta_i} T_I = \frac{\cos\theta_t}{\cos\theta_i}\frac{z_1}{z_2}|T|^2, \\ R_\Pi + T_\Pi &= 1. \end{aligned} \tag{2.5}$$

2.1 Normal incidence

For normal incidence $\theta_i = 0$, the reflection and transmission coefficients become

$$\begin{aligned} R &= \frac{1 - z_1/z_2}{1 + z_1/z_2}, \\ T &= 1 + R = \frac{2}{1 + z_1/z_2}, \\ R_\Pi &= R_I = R^2 = \left(\frac{1 - z_1/z_2}{1 + z_1/z_2}\right)^2, \\ T_\Pi &= T_I = \frac{z_1}{z_2}T^2 = \frac{4(z_1/z_2)}{(1 + z_1/z_2)^2}. \end{aligned} \tag{2.6}$$

For normal incidence the reflection and transmission coefficients are always real, and the degree of reflection and transmission only depends on the impedance mismatch z_1/z_2. We will consider five relevant cases. The reflection and transmission coefficients are shown in Fig. 2.2. Note that all the reflection and transmission coefficients are real numbers. Negative values are interpreted as a phase change of 180° compared to the incident wave.

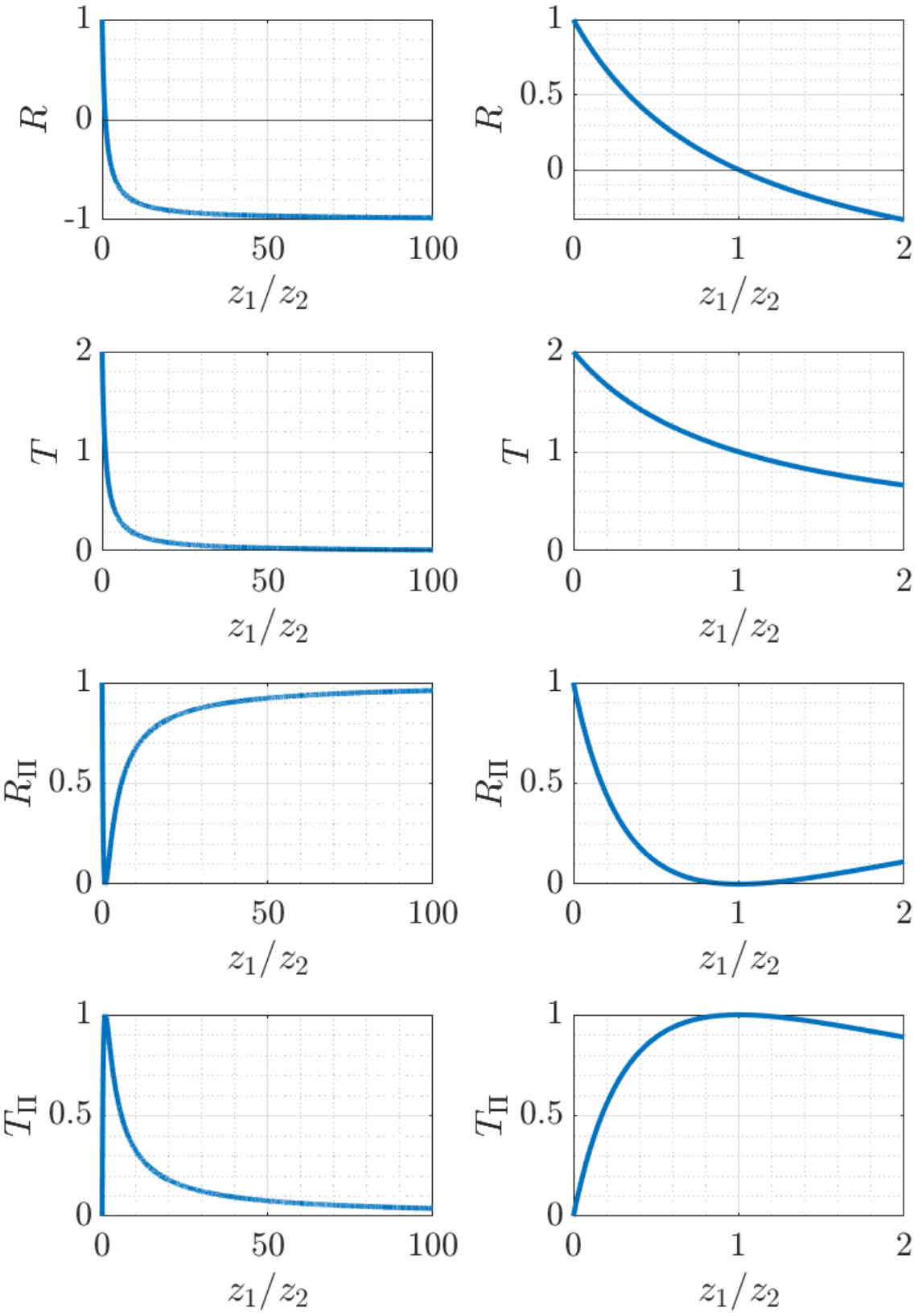

Figure 2.2 The reflection and transmission properties as a function of impedance mismatch for normal incidence.

2.1.1 Case 1: Transparent interface

In this case the impedances are equal, $z_1 = z_2$, so the interface is transparent. The reflection and transmission properties are

$$\begin{aligned} R_\Pi &= R_I = R^2 = 0, \\ T_\Pi &= T_I = T^2 = 1, \end{aligned} \tag{2.7}$$

and there is zero reflection. This is intuitive because in this case region 1 is the same as region 2, and there is no interface separating them.

2.1.2 Case 2: scattering from low to high impedance

In this case $z_1/z_2 < 1$,

$$\begin{aligned} R &> 0, \\ T &> 1, \end{aligned} \tag{2.8}$$

so there is both reflection and transmission. Note that there are zero phase changes upon reflection and transmission, but the transmitted wave has a larger pressure amplitude than the incoming wave. This is still consistent with conservation of energy because $R_\Pi + T_\Pi = 1$.

2.1.3 Case 3: scattering from high to low impedance

In this case $z_1/z_2 > 1$,

$$\begin{aligned} R &< 0, \\ T &< 1, \end{aligned} \tag{2.9}$$

so there is both reflection and transmission. The reflected wave has smaller amplitude than the incoming wave, but is 180° out of phase. The transmitted wave has smaller amplitude than the incoming wave, but has the same phase.

2.1.4 Case 4: scattering from low to rigid (incompressible) medium

In this case $z_1/z_2 \ll 1$ such that $z_1/z_2 \to 0$,

$$\begin{aligned} R &= 1, \\ T &= 2, \\ R_\Pi &= 1, \\ T_\Pi &= 0. \end{aligned} \tag{2.10}$$

This example describes e.g. an air-water interface where the sound wave travels through the air and is reflected from the water surface. The wave does not enter the rigid medium, but is totally reflected with the same phase as the incident wave. This leads to that the pressure in region 1 is doubled. The interpretation of Eq. (2.1) in region 2 is that the wavelength becomes infinite (because the speed of sound is infinite), such that the pressure is a completely flat function of position x.

2.1.5 Case 5: scattering from a free surface

In this case $z_1/z_2 \gg 1$ such that $z_1/z_2 \to \infty$,

$$\begin{aligned} R &= -1, \\ T &= 0, \\ R_I &= 1, \\ T_I &= 0. \end{aligned} \tag{2.11}$$

This example describes e.g. an water-air interface where the sound wave travels through the water and is reflected from the water surface. The incoming wave is completely reflected with a 180° phase change. The pressure at the interface is always zero to match the atmospheric pressure.

2.2 Oblique incidence

The case for oblique incidence where $\theta_i \neq 0$ is slightly more complicated. Firstly, the law of refraction results in the so-called critical angle

$$\theta_c = \arcsin\left(\frac{c_1}{c_2}\right). \tag{2.12}$$

The critical angle only exists when $c_1/c_2 < 1$. In the case when the angle of incidence is larger than the critical angle the transmitted wave becomes evanescent. That is for the case $\theta_i > \theta_c$ we have

$$\begin{aligned} p_t &= P_t e^{i(\omega t - k_1 y \sin\theta_i)} e^{-\gamma x}, \\ \gamma &= k_2 \sqrt{\left(\frac{c_2}{c_1}\right)^2 \sin^2\theta_i - 1}, \end{aligned} \tag{2.13}$$

where γ is the decay length. Note that the evanescent wave only propagates parallel to the interface, and decays perpendicular to the interface. Therefore the evanescent wave does not carry energy into medium 2 which means that $T_\Pi = 0$ for incidence angles larger than the critical angle. Secondly, there is the so-called angle of intromission θ_I which is characterised by perfect transmission and is given by

$$\sin\theta_I = \sqrt{\frac{(z_2/z_1)^2 - 1}{(z_2/z_1)^2 - (c_2/c_1)^2}}. \tag{2.14}$$

The angle of intermission can only exist when Eq. (2.14) is real.

In summary, for oblique incidence there are four cases to consider whose reflection and transmission coefficients are shown in Fig. 2.3:

1. If $c_2/c_1 < 1$ and $z_2/z_1 < 1$, there is no critical angle or angle of intromission.
2. If $c_2/c_1 < 1$ and $z_2/z_1 > 1$, then there is only an angle of intromission.
3. If $c_2/c_1 > 1$ and $z_2/z_1 > 1$, there is only a critical angle.
4. If $c_2/c_1 > 1$ and $z_2/z_1 < 1$, then there is one angle of intromission and one critical angle. The critical angle is always larger than the angle of intromission.

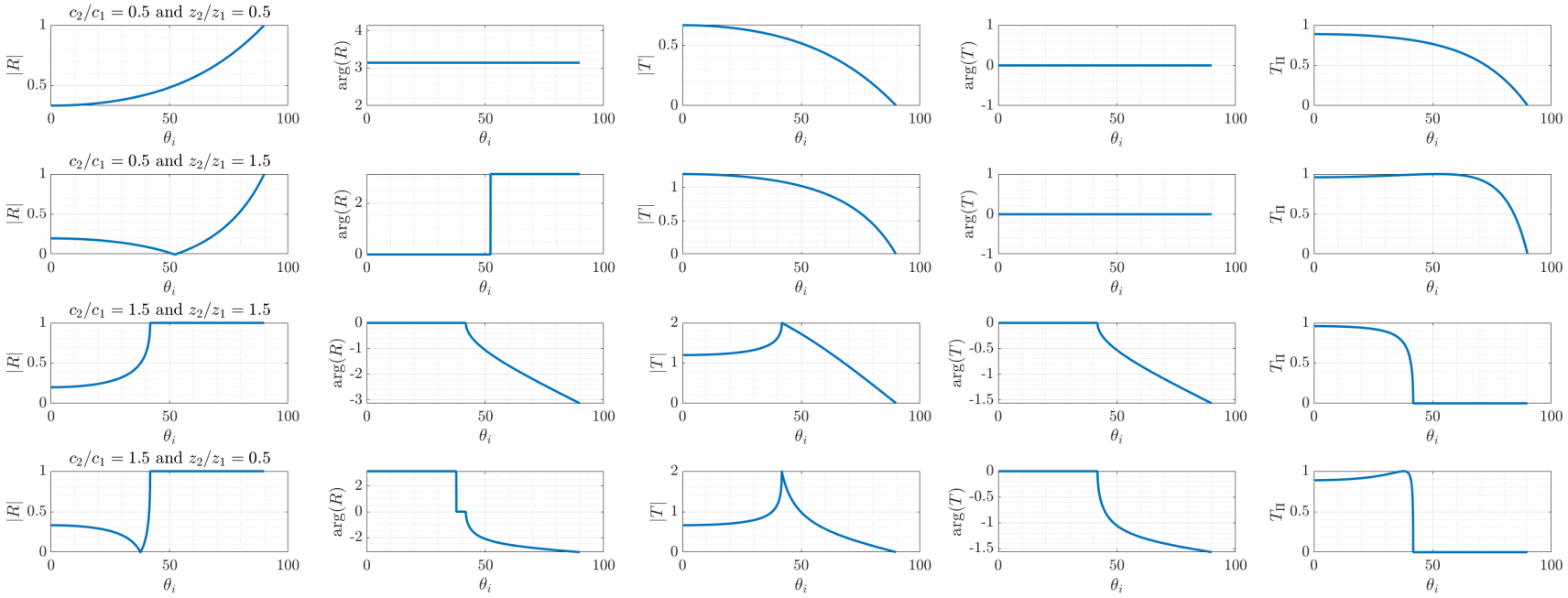

Figure 2.3 The reflection and transmission properties as a function of angle of incidence. Each row correspond to case 1-4 which are described below Eq. (2.14)*. The columns in a specific row display different scattering properties for the same case.*

2.3 Interface between water and air

For water and air, the density, speed of sound, and impedance are:

$$\rho_{\text{air}} = 1.2\,\text{kg/m}^3, \qquad \rho_{\text{water}} = 1000\,\text{kg/m}^3,$$
$$c_{\text{air}} = 340\,\text{m/s}, \qquad c_{\text{water}} = 1500\,\text{m/s},$$
$$z_{\text{air}} = 408\,\text{kg/m}^2\text{s}, \qquad z_{\text{water}} = 1.5 \times 10^6\,\text{kg/m}^2\text{s}.$$

We can use these values to compute the reflection and transmission coefficients for i) an air-water interface for a sound wave travelling in air that hits the ocean surface and ii) a water-air interface for a sound wave travelling in water and hits the ocean surface. The results are shown in Fig. 2.3.

For the air-water interface there is a critical angle of $\theta_c = 13.1°$ and no angle of intromission. Thus for angles of incidence larger than 13.1°, an evanescent wave is formed close to the interface. The impedance ratio is very small $z_{\text{air}}/z_{\text{water}} \ll 1$ which means that even for incidence angles smaller than the critical angle most of the sound wave is reflected. The wave is reflected without a phase change for most of the incident angles.

For the water-air interface there is neither a critical angle or an intromission angle. Due to the large impedance mismatch most of the wave is reflected, but because $z_{\text{water}}/z_{\text{air}} \gg 1$ there is a 180° phase change between the incident and reflected wave.

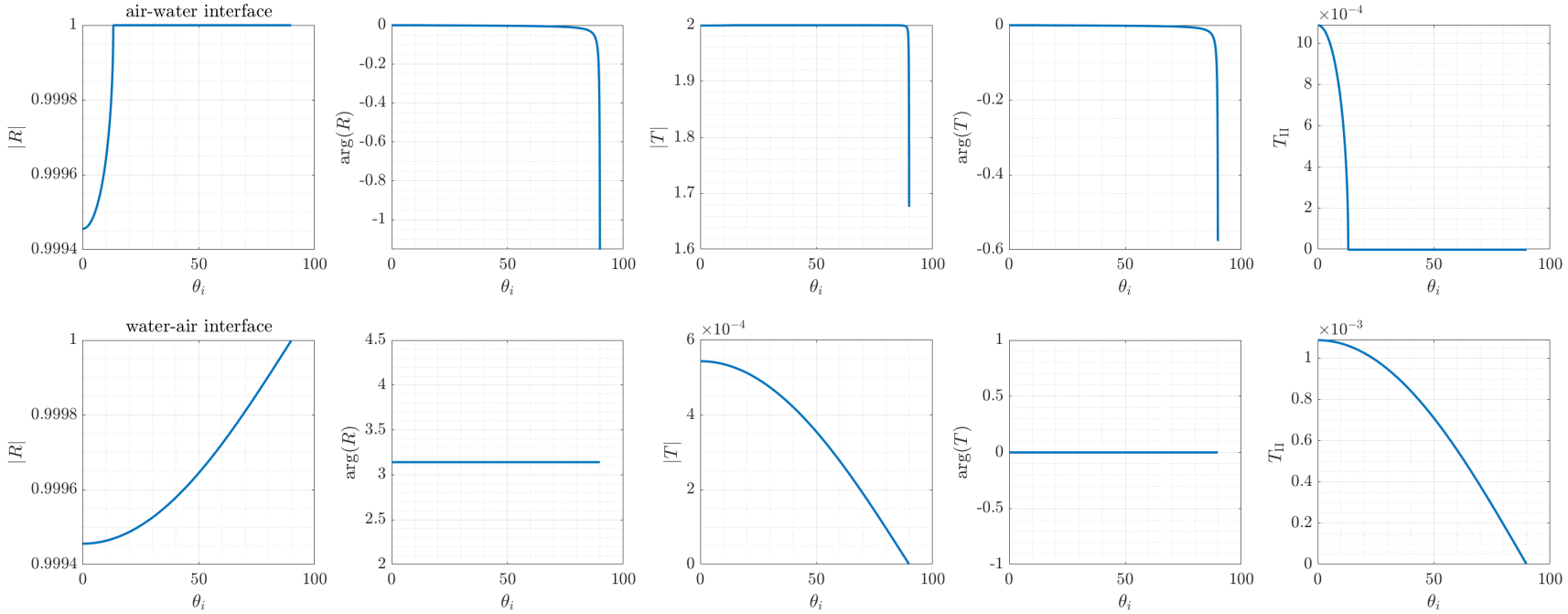

Figure 2.4 The reflection and transmission properties as a function of angle of incidence. The first and second row corresponds to the air-water and water-air interfaces respectively. The columns in a specific row display different scattering properties.

3 Trilayer scattering

The theory presented here closely follows [3, 4]. The scattering solutions discussed in the previous chapter can straightforwardly be extended to the case of a trilayer as shown in Fig. 3.1. An incident sound wave from medium 1, is reflected back into medium 1, and transmitted through the barrier to medium 3. If medium 1 and 3 are both water, this setup can be used to investigate the sound scattering properties of a barrier placed in water. We will first consider the general case where medium 1, 2, and 3 are different.

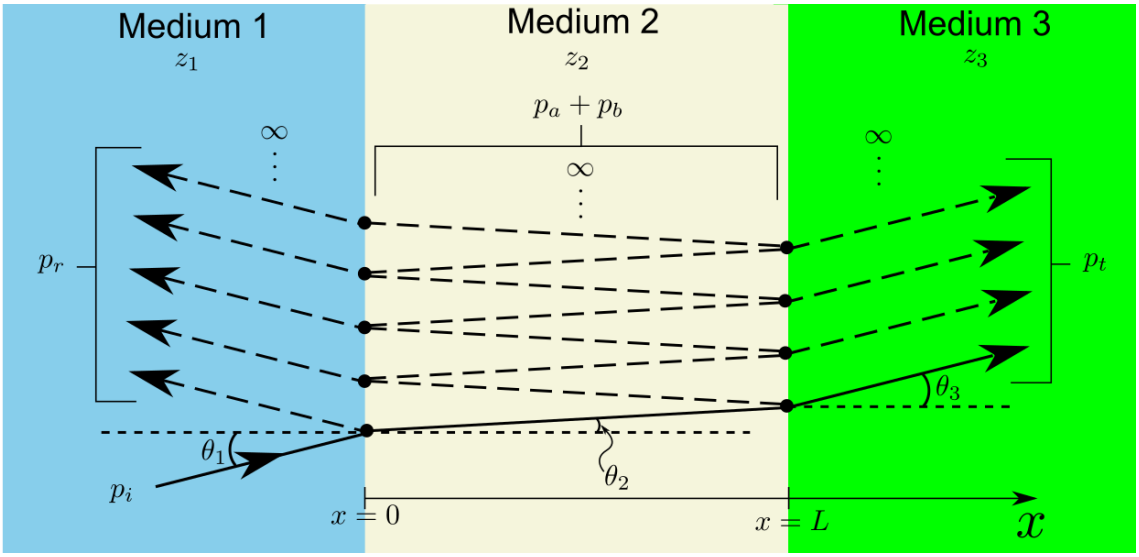

Figure 3.1 An illustration of the sound scattering problem for a trilayer.

We assume that the incoming wave originates in material 1 with angular frequency ω and wavenumber k_1. The solution ansatz[1] for oblique incidence is

$$
\begin{aligned}
p_i &= P_i e^{i(\omega t - k_1 x\cos\theta_1 - k_1 y \sin\theta_1}, \\
p_r &= P_r e^{i(\omega t + k_1 x\cos\theta_1 - k_1 y \sin\theta_1}, \\
\\
p_a &= A e^{i(\omega t - k_2 x\cos\theta_2 - k_2 y \sin\theta_2}, \\
p_b &= B e^{i(\omega t + k_2 x\cos\theta_2 - k_2 y \sin\theta_2}, \\
\\
p_t &= P_t e^{i(\omega t - k_3 x\cos\theta_3 - k_3 y \sin\theta_3}.
\end{aligned}
\tag{3.1}
$$

The corresponding boundary conditions are pressure and normal velocity continuity at both of the interfaces:

1. Pressure continuity at $x = 0$: $P_i + P_r = A + B$.
2. Normal velocity continuity at $x = 0$: $\frac{P_i - P_r}{Z_1} = \frac{A-B}{Z_2}$

[1] Alternatively the trilayer scattering problem can be expressed as an infinite geometric sum where each summand is a bilayer scattering problem as shown in Fig. 3.1. The geometric-sum method gives the same answer as the ansatze in Eq. 3.1, but superficially the calculation looks more complicated. The geometric-sum method is illustrated in [4].

3. Pressure continuity at $x = L$: $Ae^{-i\kappa_2 L} + Be^{i\kappa_2 L} = P_t e^{-i\kappa_3 L}$.
4. Normal velocity continuity at $x = L$: $\frac{Ae^{-i\kappa_2 L} - Be^{i\kappa_2 L}}{Z_2} = \frac{P_t e^{-i\kappa_3 L}}{Z_3}$.

To simplify the notation we have here defined $\kappa_j = k_j \cos\theta_j$ and $Z_j = z_j/\cos\theta_j$ where $j = \{1, 2, 3\}$. If we insert the ansatze into the boundary conditions, we find that the reflection and transmission coefficient become

$$\begin{aligned} R &= \frac{P_r}{P_i} = \frac{\left(1 - \frac{Z_1}{Z_3}\right)\cos\kappa_2 L + i\left(\frac{Z_2}{Z_3} - \frac{Z_1}{Z_2}\right)\sin\kappa_2 L}{\left(1 + \frac{Z_1}{Z_3}\right)\cos\kappa_2 L + i\left(\frac{Z_2}{Z_3} + \frac{Z_1}{Z_2}\right)\sin\kappa_2 L}, \\ T &= \frac{P_t}{P_i} = \frac{2e^{i\kappa_3 L}}{\left(1 + \frac{Z_1}{Z_3}\right)\cos\kappa_2 L + i\left(\frac{Z_2}{Z_3} + \frac{Z_1}{Z_2}\right)\sin\kappa_2 L}. \end{aligned} \tag{3.2}$$

The boundary conditions also give us the law of refraction (Snell's law) on the form

$$\frac{\sin\theta_1}{c_1} = \frac{\sin\theta_2}{c_2} = \frac{\sin\theta_3}{c_3} \tag{3.3}$$

as well as the law of reflection at each interface. The critical angle for the 1-2 and 2-3 interfaces are $\theta_{1,c} = \arcsin(c_1/c_2)$ and $\theta_{2,c} = \arcsin(c_2/c_3)$ respectively. If $\theta_j > \theta_{j,c}$, $(j = \{1, 2\})$ we obtain evanescent solutions. In the limit where there is no barrier ($L \to 0$) we recover the reflection and transmission coefficient for the bilayer configuration.

3.1 The scattering properties of a water-barrier-water system

To study the effect of a barrier placed in water we will assume that region 1 and 3 consists of water. In that case the impedance and sound speed of region 1 and 3 are identical. Also, the angle of incidence in material 1 is equal to the angle of emergence in material 3, $\theta_1 = \theta_3$. The reflection and transmission coefficients in Eq. (3.2) then simplify to

$$\begin{aligned} R &= \frac{i\left(\frac{Z_2}{Z_1} - \frac{Z_1}{Z_2}\right)\sin\kappa_2 L}{2\cos\kappa_2 L + i\left(\frac{Z_2}{Z_1} + \frac{Z_1}{Z_2}\right)\sin\kappa_2 L}, \\ T &= \frac{2e^{i\kappa_1 L}}{2\cos\kappa_2 L + i\left(\frac{Z_2}{Z_1} + \frac{Z_1}{Z_2}\right)\sin\kappa_2 L}. \end{aligned} \tag{3.4}$$

From the reflection coefficient we can deduce that there are certain frequencies that will be perfectly reflected from the barrier and certain frequencies that will be (imperfectly) transmitted through the barrier. These frequencies follows by solving the equations $\sin\kappa_2 L = 0$ and $\sin\kappa_2 L = \pm 1$ respectively. The transmitted and reflected frequencies are given by

$$\begin{aligned} f_T &= n\pi\tilde{f}, \\ f_R &= (n + 1/2)\pi\tilde{f}, \end{aligned} \tag{3.5}$$

respectively. In the above $n\,(=0,1,2,3),\ldots$ is a non-negative integer. The reflected and transmitted frequencies are defined in units of the intrinsic frequencies which are

$$\begin{aligned}\tilde{f} &= \frac{f_0}{2\pi\sqrt{\left(\frac{c_1}{c_2}\right)^2 - \sin^2\theta_1}},\\ f_0 &= c_1/L.\end{aligned} \tag{3.6}$$

Note that the characteristic frequency $\tilde{f}$ is defined by the natural frequency f_0, the speed of sound ratio, and the angle of incidence.

Another no-reflection condition follows from solving $Z_2/Z_1 - Z_1/Z_2 = 0$, which is equivalent to solving the equation

$$\frac{z_2}{z_1}\cos\theta_1 = \sqrt{1 - \left(\frac{c_2}{c_1}\right)^2 \sin^2\theta_1}. \tag{3.7}$$

The equation only has a solution for the angle of incidence when either

$$\begin{aligned}&c_2/c_1 > 1 \text{ and } z_2/z_1 < 1 \text{ or}\\ &c_2/c_1 < 1 \text{ and } z_2/z_1 > 1.\end{aligned} \tag{3.8}$$

For conventional materials, Eq. (3.8) is difficult to satisfy because typically, the more dense a material is the higher its speed of sound.

To study the transmission through a barrier it is convenient to also use the transmission power coefficient. This is because i) it is a single real number (does not take the relative phases into account), ii) evanescent states does not contribute to the energy flow, and iii) energy conservation is manifest through the relationship $T_\Pi + R_\Pi = 1$. The reflection and transmission power coefficients are given by

$$\begin{aligned}R_\Pi = |R|^2 &= \frac{\left(\frac{Z_2}{Z_1} - \frac{Z_1}{Z_2}\right)^2 \sin^2\left(f/\tilde{f}\right)}{4\cos^2\left(f/\tilde{f}\right) + \left(\frac{Z_2}{Z_1} + \frac{Z_1}{Z_2}\right)^2 \sin^2\left(f/\tilde{f}\right)},\\ T_\Pi = |T|^2 &= \frac{4}{4\cos^2\left(f/\tilde{f}\right) + \left(\frac{Z_2}{Z_1} + \frac{Z_1}{Z_2}\right)^2 \sin^2\left(f/\tilde{f}\right)}.\end{aligned} \tag{3.9}$$

In Fig. 3.2 we have plotted the transmission power coefficient T_Π as an independent function of $f/\tilde{f}\,(=\kappa_2 L)$ and Z_2/Z_1. The former represents the effective barrier length compared to the wavelength inside the barrier, and the latter represent the effective impedance mismatch. Here the word effective refers to that both quantities are also dependent on the angle of incidence.

The transmission power coefficient depends on the effective impedance mismatch Z_2/Z_1. The more dissimilar the impedance of the barrier is from water the more the transmission properties are suppressed. Close to zero impedance mismatch $Z_2/Z_1 = 1$, there is a plateu of perfect transmission. The transmission power coefficient is a periodic function of $f/\tilde{f}$, with minima and maxima given by $f/\tilde{f} = (n+1/2)\pi$ and $f/\tilde{f} = n\pi$ respectively. The maxima are not suppressed even for dissimilar effective impedance mismatch Z_2/Z_1. In order for the barrier to protect effectively against sound it needs to have an impedance significantly different from water, i.e. either $Z_2/Z_1 \ll 1$ or $Z_2/Z_1 \gg 1$. The transmission of such materials is still a function of $f/\tilde{f}$, but it is possible to somewhat tune $\tilde{f}$ by changing e.g. the barrier length, angle of incidence, or the speed of sound ratio. We will give some examples of this in terms of a bubble curtain in Sec. 3.3.

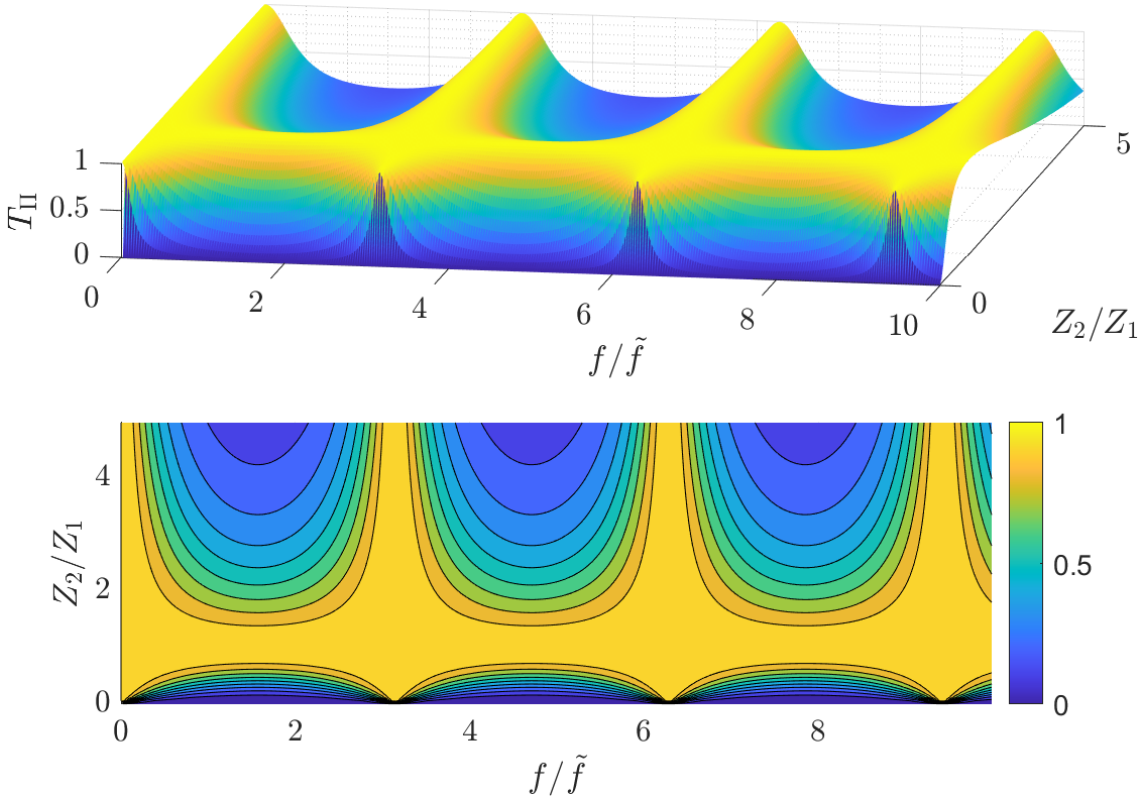

Figure 3.2 The transmission power coefficient as an independent function of frequency and impedance mismatch.

3.2 A simplified bubble curtain

The simplest model to describe a bubble curtain is to assume an ideal two-component model where the water is in a continuous phase and the gas is in a disperse phase. The discussion here is based on the books written by Brennen [5] and Wood [6]. The model for a bubbly liquid is sometimes called Wood's model. For an ideal mix between water and air, the density and speed of sound is

$$\begin{aligned} \rho_m &= \alpha\rho_g + (1-\alpha)\rho_l, \quad \text{and} \\ c_{\mathrm{m}} &= \frac{1}{\sqrt{\left[\rho_l\left(1-\alpha\right)+\rho_g\alpha\right]\left[\frac{\alpha}{kp}+\frac{1-\alpha}{\rho_l c_l^2}\right]}}, \end{aligned} \tag{3.10}$$

respectively. The relative volume fraction of the gas is denoted by α. The subindices m, g, and l refers to the mix (bubble curtain), gas (air), and liquid (water) respectively. The process can be either isothermal ($k = 1$) or adiabatic ($k = \gamma = 1.4$) where γ is the adiabatic constant. In the cases $\alpha = 0$ (only water) and $\alpha = 1$ (only air) the speed of sound becomes equal to the speed of sound of water and air respectively.

We also need to specify how the parameters depend on water depth. Since, a bubble curtain can not be placed in very deep water, as the bubbles will be too compressed, we will assume that the water properties are constant, i.e. $c_L = 1500\,\mathrm{m/s}$ and $\rho_L = 1000\,\mathrm{kg/m^3}$. The hydrostatic pressure is given by the standard expression $p = p_{\mathrm{atm}} + \rho_l g z$, where p_{atm}, g, and z are the atmospheric pressure, acceleration of gravity, and water depth respectively. On the other hand, we will assume that the air acts as an ideal gas. The ideal gas speed of sound and density is given by $c = \sqrt{kRT} = \sqrt{kp/\rho_G}$ and $\rho_G = (A_k p)^{1/k}$. The constant A_k is determined by specifying the gas constant R and temperature T. For $R = 280\,\mathrm{m^2/s^2K}$ and $T = 293\,\mathrm{K}$ we obtain

$$A_k = \begin{cases} 1.22\times10^{-5}, & k = 1 \text{ (Isothermal)} \\ 1.33\times10^{-5}, & k = 1.4 \text{ (Adiabatic)}. \end{cases} \tag{3.11}$$

In Fig. 3.3 we have plotted the bubble curtain properties as a function of the volume fraction of air. For the qualitative purposes discussed here the differences between $k = 1.4$ and $k = 1$ are negligible. Note that the speed of sound inside of the bubble curtain can be much smaller than both the speed of sound of pure water and pure air. In addition, the speed of sound is a relatively flat function of α for a large parameter regime. This means that for sound that come from the water and hit the bubble curtain there is no critical angle. In addition, the relative impedance mismatch between the bubble curtain and water is also smaller than unity, and decreases with the volume fraction of air. Consequently, the transmission power function lies in the regime close to the $f/\tilde{f}$-axis in the phase diagram of Fig. 3.2. Hence, the bubble curtain is able to strongly reflect sound but there will be oscillations with the frequency parameter $f/\tilde{f}$.

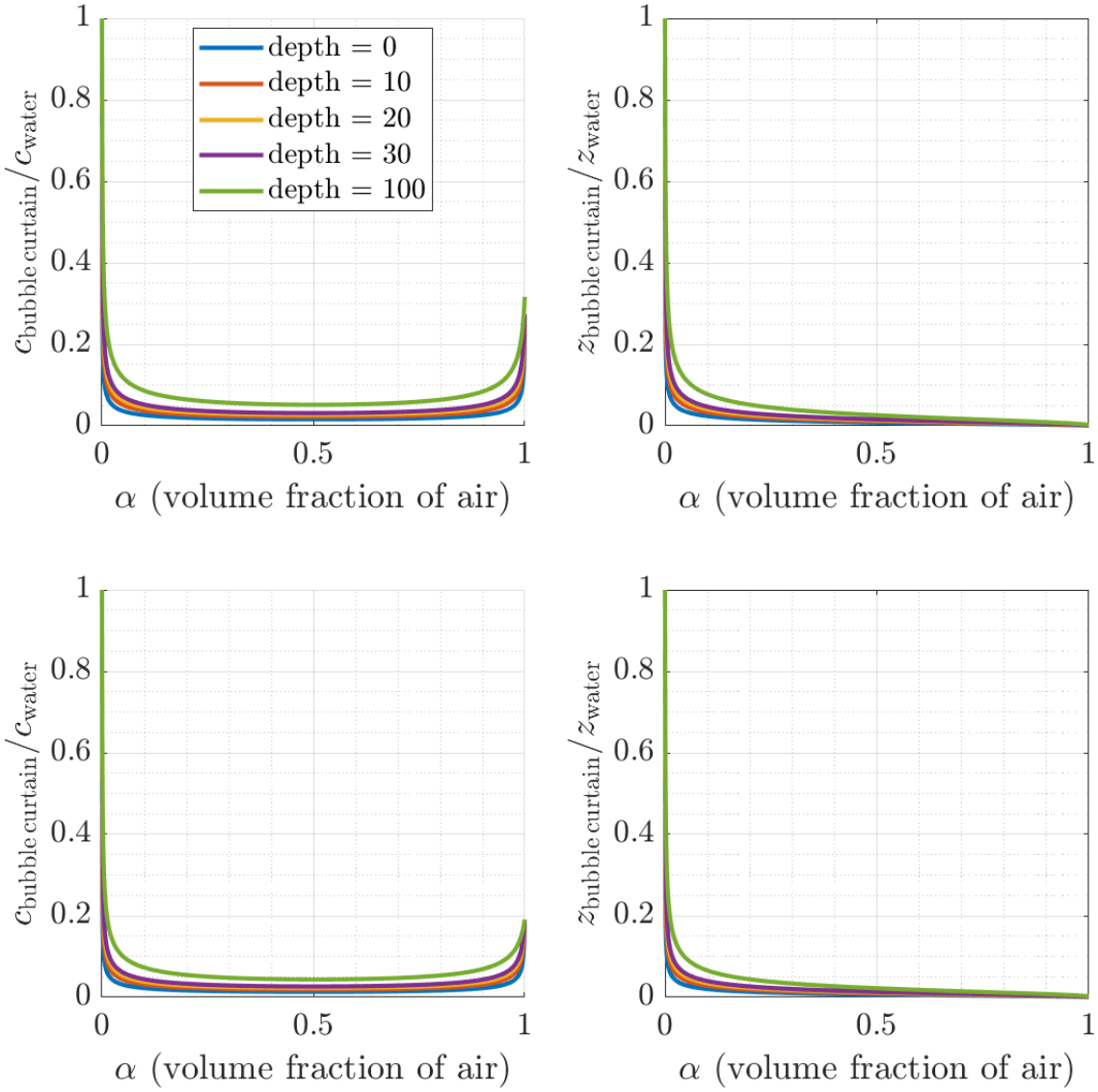

Figure 3.3 The speed of sound and impedance in the bubble curtain relative to water as a function of the amount of volume occupied by the air bubbles. The first and second row corresponds to $k = 1.4$ (adiabatic) and $k = 1$ (isothermal).

3.3 Examples of bubble curtain protection

The application of the scattering theory to describe a bubble curtain has been previously discussed in [7]. In this report we have significantly extended the analysis, and description of the bubble curtain. In this section we will plot the transmission power amplitude for a variety of bubble-curtain examples. A Matlab program which calculates the transmission properties of a bubble curtain are given in App. A. We will consider a broad frequency range $f = 0 - 1.6\,\text{MHz}$ and all possible angles of incidence $\theta_1 = (0, \pi/2)$. For conevience we set the length of the barrier $L = 1\,\text{m}$. Furthermore, the bubble curtain will have either little ($\alpha = 0.03$) or much ($\alpha = 0.3$) air bubbles. We will consider bubble curtains located at the depths $z = 10\,\text{m}$, $z = 30\,\text{m}$, and $z = 100\,\text{m}$. In reality for the case $z = 100\,\text{m}$, the bubble curtain is likely not functional due to the large hydrostatic pressure, but it is included to emphasize mathematical trends. We plot the transmission power amplitude as a contour plot with the frequency f and angle of incidence θ_1 as variables. All of the examples are plotted in Figs. 3.4-3.9.

First we will consider the general features of the figures. Note that all the figures contain colored bands (which may be vertical or curved), where the transmission amplitude is close to unity. The central frequency of these bands are given by $f = n\pi\tilde{f}$, $n = (0, 1, 2, \dots)$. We will refer to these bands as the bands of perfect transmission. For small frequencies the bands of perfect transmission are vertical, which means that they are relatively independent of the angle of incidence. As the frequency increases the bands of perfect transmission becomes curved, i.e. very dependent on the angle of incidence. We can understand this physically by recalling that the relationship between frequency and wavelength is inversely proportional. For small frequencies, the wavelength is much larger than both the barrier and the bubbles, irrespective of the angle of incidence. Hence, the number of oscillations that occur inside the barrier are not very dependent on the angle of incidence. For large frequencies, the wavelength is very small compared to the barrier. Hence, the sound wave oscillates and interacts with the barrier many times. For the high frequency case, the length (and therefore the number of oscillations) that the sound wave travels through the barrier is strongly dependent on the angle of incidence. Therefore the interaction becomes highly dependent on the angle of incidence. The net effect is that for small frequencies a lot of the signal is completely reflected, but for larger frequencies the bubble curtain provides less protection unless the angle of incidence is small.

In Figs. 3.4-3.6 we consider a bubble curtain with 3% air bubbles at increasing depth. Note that the general features just discussed are still present. The new effect is that the thickness of the bands of perfect transmission (the vertical and curved spikes) increases with depth. This can be explained by the increasing hydrostatic pressure in combination with the small amount of air. For increasing depths the bubble curtain basically begins to behave more and more like the surrounding water, which means that the impedance mismatch decreases. Hence, the bubble curtain looses some of its reflection properties.

In Figs. 3.7-3.9 we consider a bubble curtain with 30% air bubbles at increasing depth. In this case, since there is much more air present, the bubble curtain does not begin to behave similarly to water unless the depth is very large. Therefore the widths of the bands of perfect transmission only slightly increases with depth.

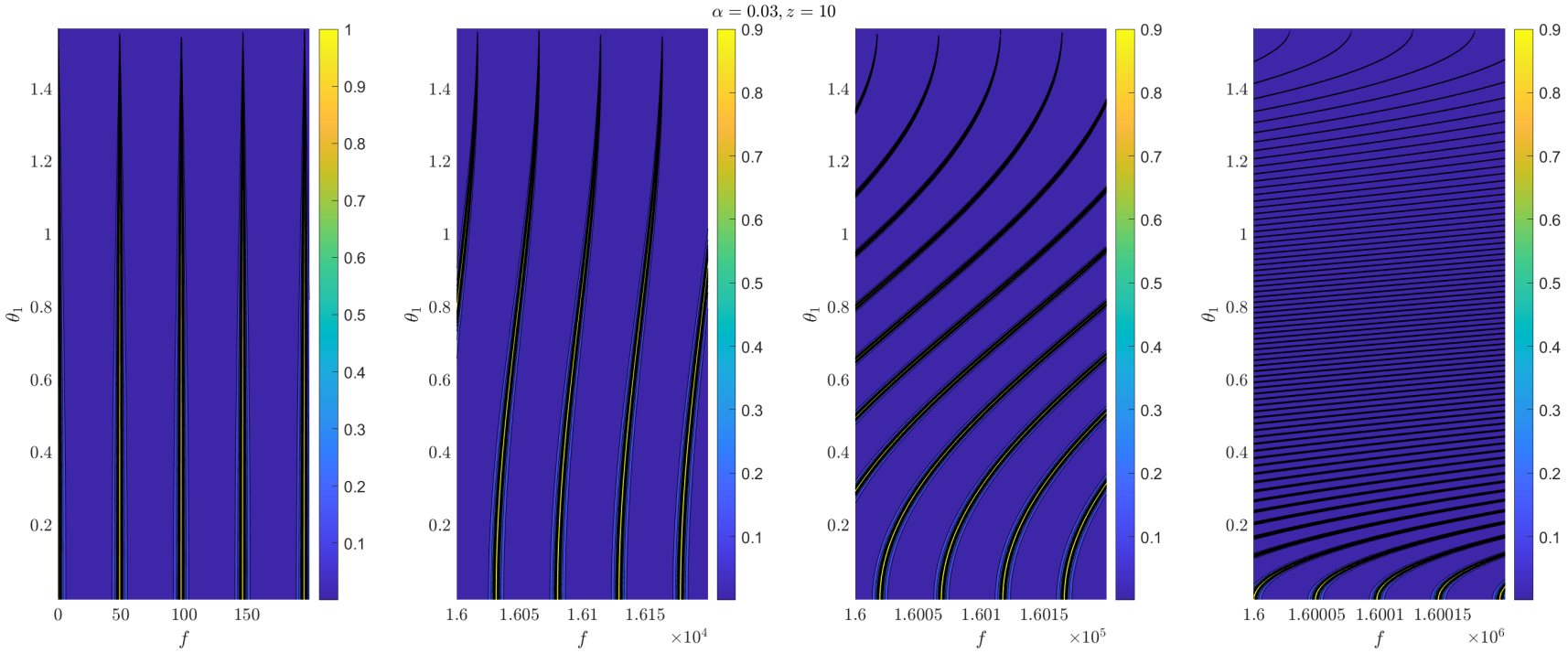

Figure 3.4 The transmission power coefficient vs frequency and angle of incidence for a bubble curtain with 3% air and at a depth of 10 m.

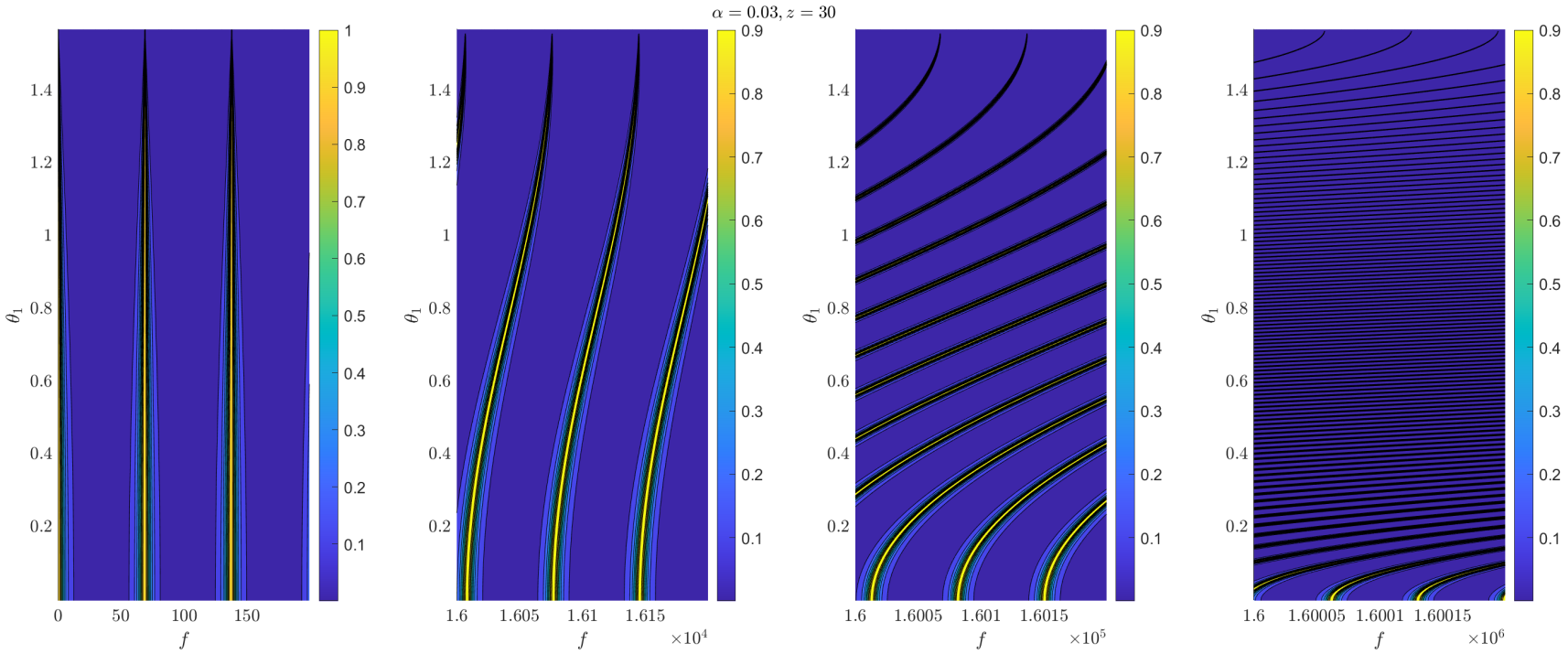

Figure 3.5 The transmission power coefficient vs frequency and angle of incidence for a bubble curtain with 3% air and at a depth of 30 m.

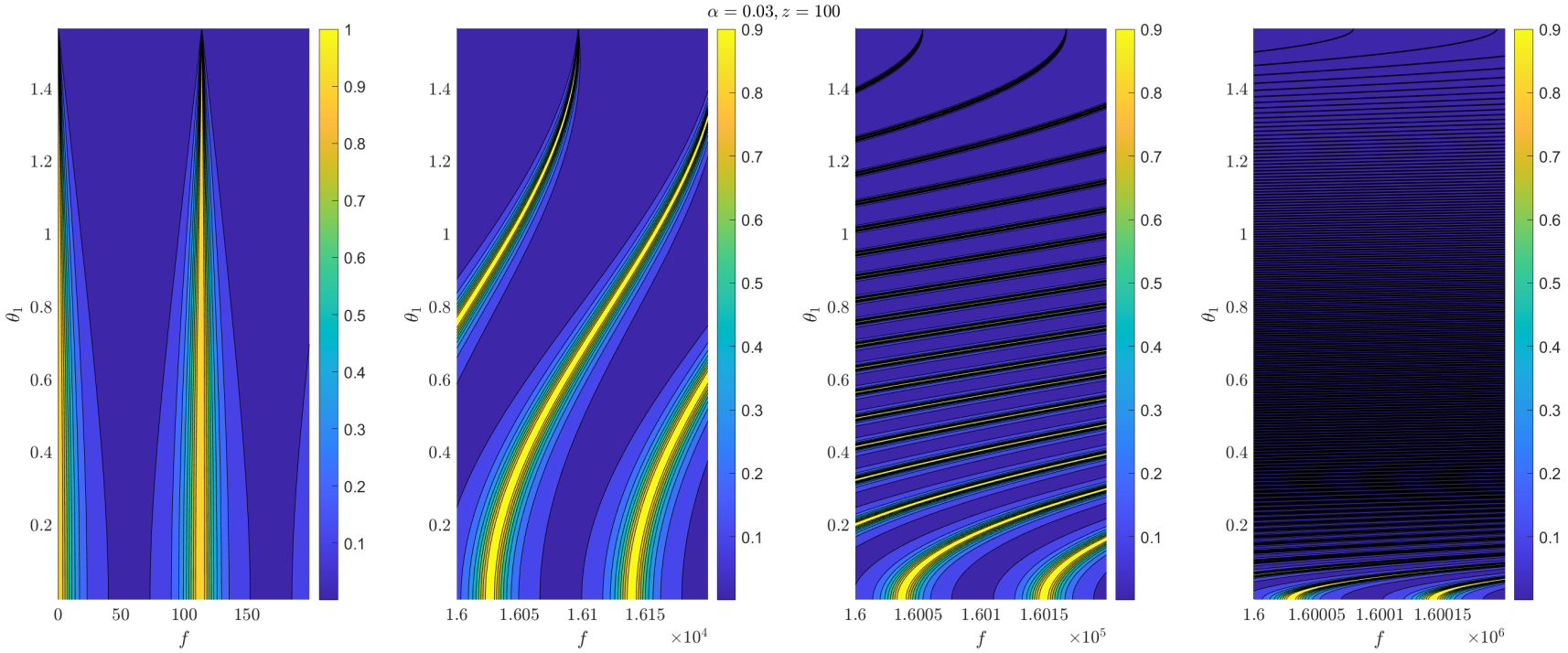

Figure 3.6 The transmission power coefficient vs frequency and angle of incidence for a bubble curtain with 3% air and at a depth of 100 m.

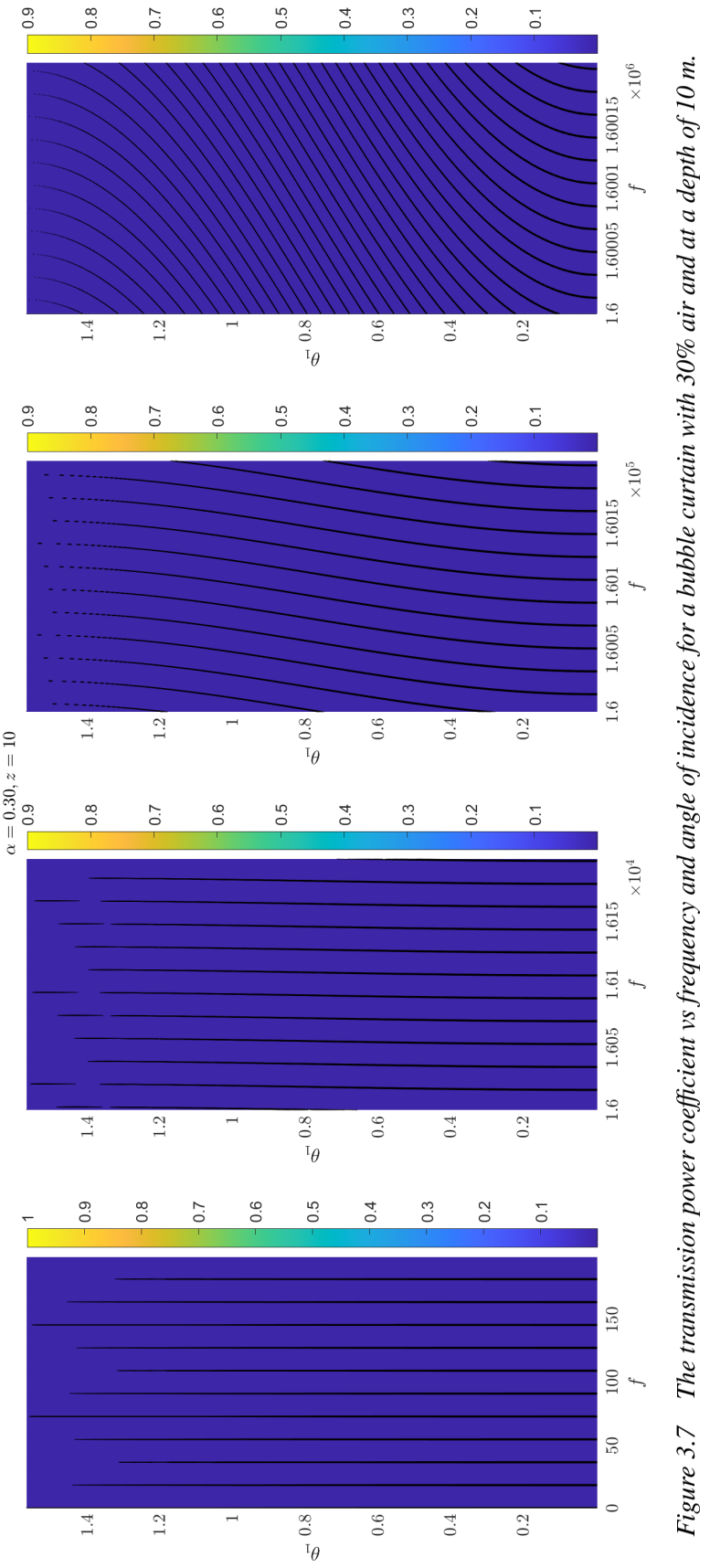

Figure 3.7 The transmission power coefficient vs frequency and angle of incidence for a bubble curtain with 30% air and at a depth of 10 m.

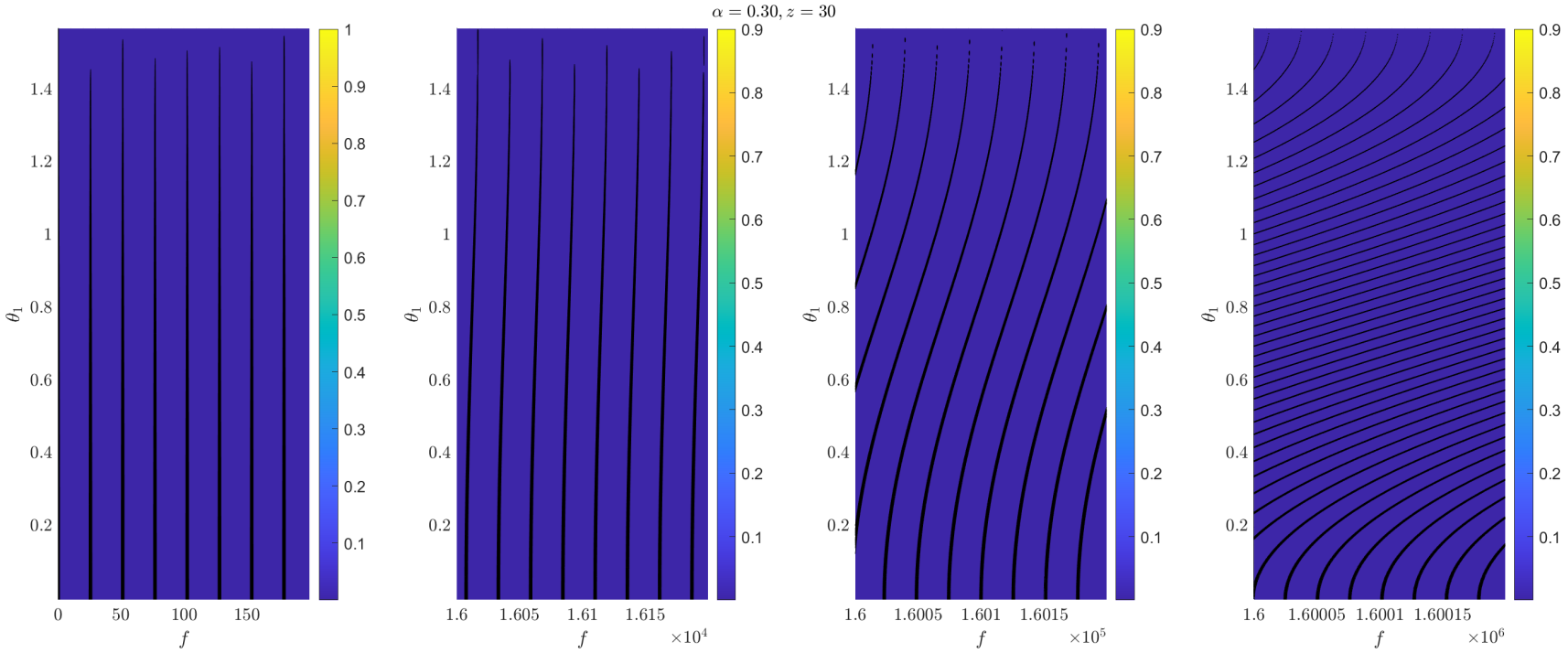

Figure 3.8 The transmission power coefficient vs frequency and angle of incidence for a bubble curtain with 30% air and at a depth of 30 m.

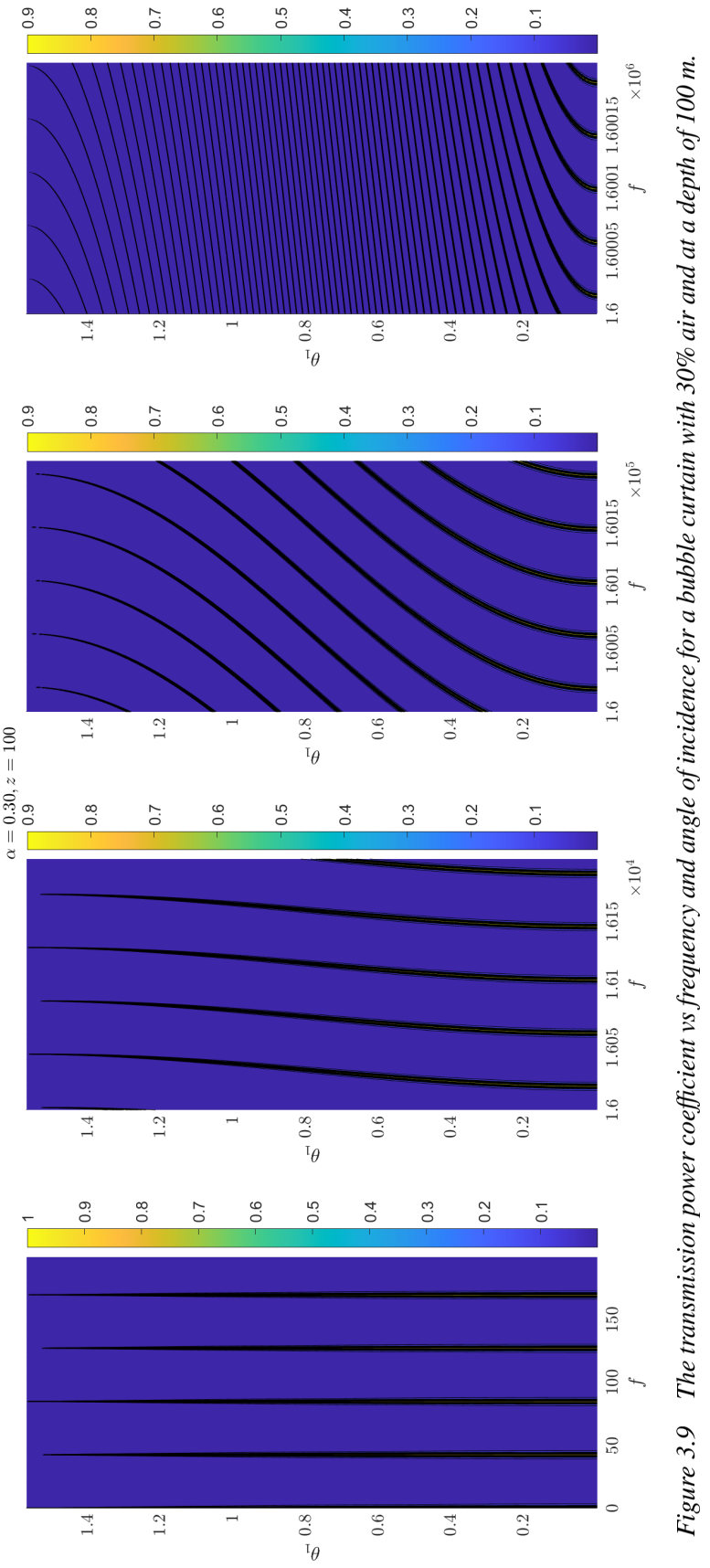

Figure 3.9 The transmission power coefficient vs frequency and angle of incidence for a bubble curtain with 30% air and at a depth of 100 m.

3.4 Limitations of the theory and possible extensions

In the theory we have presented here the bubble curtain is treated as an ideal two-phase medium specified by an uniform impedance and speed of sound. In reality, the bubble curtain contains the following properties:

- The bubbles are not distributed uniformly.
- As the bubbles move upward due to buoyancy, they increase in size due to the lower hydrostatic pressure.
- If the frequency of the incoming sound wave matches some of the bubble resonance frequencies bubble dynamics will be initiated.

The non-uniform distribution of the bubbles are important when the sound wave's wavelength inside of the bubble curtain is comparable to the bubble radii. If we view the bubble screen as a disordered medium then we expect (weak) Anderson localization to occur (in 3D). Anderson localization typically manifests itself in a scattering problem as an exponential damping. Without working out the computational details it is difficult to determine the damping length scale. An upper threshold on the frequencies where we expect Anderson localization to occur is given by $f_A = c_m/r$ where r is the bubble radius. For sound waves with frequencies close to f_A, the disordered bubble structure will lead to additional damping. In Tab. 3.1 we compute some values of f_A.

An additional damping mechanism comes from the bubble dynamics. The bubble dynamics are important when the frequency of the sound wave coincides with the resonance frequency of the bubbles. A simple estimate for the bubble resonance frequency is given by the Minnaert resonance formula [8]

$$f_r = \frac{1}{2\pi r}\sqrt{\frac{3\gamma p}{\rho_L}}. \tag{3.12}$$

Examples of the bubble resonance frequencies are given in Tab. 3.2.

The classical scattering theory which we have just described is therefore expected to over-predict the transmission for frequencies larger than those in Tab. 3.1 and close to those of Tab. 3.2. However, the theory is useful to determine a concrete upper bound on the degree of damping that does not depend on difficult-to-measure bubble properties such as the individual bubble configuration.

Table 3.1 Frequencies f_A where the disordered bubble structure leads to additional damping. The frequencies are given in kHz.

		Bubble radius [mm]				
		5	10	20	30	40
Speed of sound [m/s]	100	20	10	5	3.3	2.5
	40	8	4	2	1.3	1
	20	4	2	1	0.7	0.5

Table 3.2 Resonance frequencies f_R where the bubble dynamics lead to additional damping. The frequencies are given in kHz.

		Bubble radius [mm]				
		5	10	20	30	40
Depth [m]	10	0.92	0.46	0.23	0.15	0.12
	20	1.13	0.56	0.28	0.19	0.14
	30	1.30	0.65	0.32	0.22	0.16

4 Summary and conclusion

A bubble curtain, created by pushing compressed air through a perforated pipe under water, forms a barrier of rising air bubbles. This curtain can protect marine life from underwater noise pollution. In this report, we assess the protective capabilities of bubble curtains by developing a straightforward method to calculate the sound transmission.

Theoretically, the speed of sound in a bubble curtain can be lower than in both air and water due to that the bubbles create a highly compressible mixture. This effect is dependent on the ratio of the total air volume to the overall volume of the mixture, known as the volume fraction of air.

Because of the low sound speeds, there is a significant (acoustic) impedance mismatch between the water and the bubble curtain. Impedance, defined as the product of density and sound speed, measures how much a medium resists the flow of sound waves. The large impedance mismatch results in the bubble curtain acting as a highly reflective sound shield under the right conditions, providing substantial sound protection.

Our model indicates that bubble curtains are most effective at shielding sound frequencies up to 100 kHz, though performance varies with factors like hydrostatic pressure, bubble size, and the angle of sound waves relative to the curtain. The model shows significantly reduced performance at frequencies above 1 MHz, but it does not account for disordered localization phenomena in these ranges. Future models may offer better insights into performance at higher frequencies.

References

[1] T. C. Johannessen, A. Johnsen, O. Dullum, and B. Bjerketveit. Trykkbølgedemping ved sprengning under vann - småskalatester av boblegardin og luftfylte materialer. Technical Report 17/16837, The Norwegian Defence Research Establishment (FFI), 2017.

[2] S. N. Domenico. Acoustic wave propagation in air-bubble curtains in water-part i: History and theory. *GEOPHYSICS*, 47(3):345–353, 1982.

[3] L. E. Kinsler, A. R. Frey, A. B. Coppens, and J. V. Sanders. *Fundamentals of acoustics*. John Wiley & Sons, Inc, 2000.

[4] C. B. Officer. *Introduction to the theory of sound transmission with application to the ocean*. McGraw Hill Book Company, Inc, 1958.

[5] C. E. Brennen. *Fundamentals of Multiphase flows*. Cambridge University Press, 2005.

[6] A.B. Wood. *A Textbook of Sound: Being an Account of the Physics of Vibrations with Special Reference to Recent Theoretical and Technical Developments*. The Macmillan Company, 1957.

[7] K. W. Marr. *On the design of an acoustically isolating bubble screen for the Carr inlet acoustic range*. PhD thesis, Naval Postgraduate School, Monterey, California 93940, 1981.

[8] M. Minnaert. Xvi. on musical air-bubbles and the sounds of running water. *The London, Edinburgh, and Dublin Philosophical Magazine and Journal of Science*, 16(104):235–248, 1933.

A Matlab implementation of bubble curtain

```
%Relevant frequencies
f1 = 0:0.3:200;
f2 = (0+16000):0.3:(16000+200);
f3 = (0+160000):0.3:(160000+200);
f4 = (0+1600000):0.3:(1600000+200);

%Generate a mesh between the relevant frequencies and angle of incidence
[f1,theta1] = meshgrid(f1,0.000001:0.0006:pi/2-0.000001);
[f2,theta1] = meshgrid(f2,0.000001:0.0006:pi/2-0.000001);
[f3,theta1] = meshgrid(f3,0.000001:0.0006:pi/2-0.000001);
[f4,theta1] = meshgrid(f4,0.000001:0.0006:pi/2-0.000001);

%Determine the amount of air, water depth, and adiabatic gas constant
alpha = 0.3;
depth = 20;
gamma = 1.4;

%Calculate transmission power amplitudes
Tpi1 = globalThreeLayer(gamma, alpha, depth, f1, theta1);
Tpi2 = globalThreeLayer(gamma, alpha, depth, f2, theta1);
Tpi3 = globalThreeLayer(gamma, alpha, depth, f3, theta1);
Tpi4 = globalThreeLayer(gamma, alpha, depth, f4, theta1);

%Plot the transmission power amplitude as
%a function of angle of incidence and frequency
figure(1)
sgtitle(sprintf('$\\alpha =  %.2f, z = %.0f $', alpha, depth))
subplot(1,4,1)
hold on
contourf(f1,theta1,Tpi1)
colorbar
xlabel('$f$')
ylabel('$\theta_1$')
grid on
grid minor

subplot(1,4,2)
hold on
contourf(f2,theta1,Tpi2)
colorbar
xlabel('$f$')
ylabel('$\theta_1$')
grid on
grid minor
```

```
subplot(1,4,3)
hold on
contourf(f3,theta1,Tpi3)
colorbar
xlabel('$f$')
ylabel('$\theta_1$')
grid on
grid minor

subplot(1,4,4)
hold on
contourf(f4,theta1,Tpi4)
colorbar
xlabel('$f$')
ylabel('$\theta_1$')
grid on
grid minor


%%%%%%%%%% Necessary Functions %%%%%%%%%%

%Function to calculate the transmission power amplitude
function Tpi = globalThreeLayer(k, alpha, depth, f, theta1)

%Call the speed of sound and impedance of the bubble curtain
[c2, z2] = SoundSpeedMix(k, alpha, depth);

%Water properties
c1 = 1500;
rho1 = 1000;
c = c2./c1;
z1 = rho1*c1;

%Necessary to define cos(theta_2) through
%an analytical continuation due to complex values
costheta2 = sqrt(1 - c.^2 .* sin(theta1).^2);

%Barrier length fixed to 1 meter divided by the speed of sound in water
l = 1/1500;

%Intermediate variables
x = 2.*pi.*l.*f.*sqrt(1./c.^2 - sin(theta1).^2);
y = z2./z1.*cos(theta1)./costheta2;

%Transmission power amplitude
```

```
Tpi = 4 ./ ( 4.*cos(x).^2 + (y + 1./y).^2.*sin(x).^2);
end

%Function to calculate the speed of sound and impedance
%inside of the bubble curtain - ideal mix theory
function [cmix, impedance_mix] = SoundSpeedMix(k, alpha, z)

%k = 1 isothermal
%k = 1.4 adiabatic
if k == 1
    A = 1.22*10^(-5);
else
    A = 1.33*10^(-5);
end

%Hydrotatic pressure in water (density = 1000 kg/m^3)
rhoL = 1000;
cL = 1500;
g = 9.81;
patm = 101325;
p = patm + rhoL*g*z;

%Density of gas given a hydrostatic pressure
rhoG = (A * p).^(1./k);

%The ideal mix speed of sound, density, and impedance
cmix = 1./sqrt( (rhoL.*(1-alpha) + ...
rhoG.*alpha).*(alpha./(k*p) +...
(1-alpha)./(rhoL.*cL.^2)) );
rho_mix = alpha.*rhoG + (1-alpha).*rhoL;
impedance_mix = rho_mix .*cmix;
end
```

About FFI

The Norwegian Defence Research Establishment (FFI) was founded 11th of April 1946. It is organised as an administrative agency subordinate to the Ministry of Defence.

FFI's mission

FFI is the prime institution responsible for defence related research in Norway. Its principal mission is to carry out research and development to meet the requirements of the Armed Forces. FFI has the role of chief adviser to the political and military leadership. In particular, the institute shall focus on aspects of the development in science and technology that can influence our security policy or defence planning.

FFI's vision

FFI turns knowledge and ideas into an efficient defence.

FFI's characteristics

Creative, daring, broad-minded and responsible.

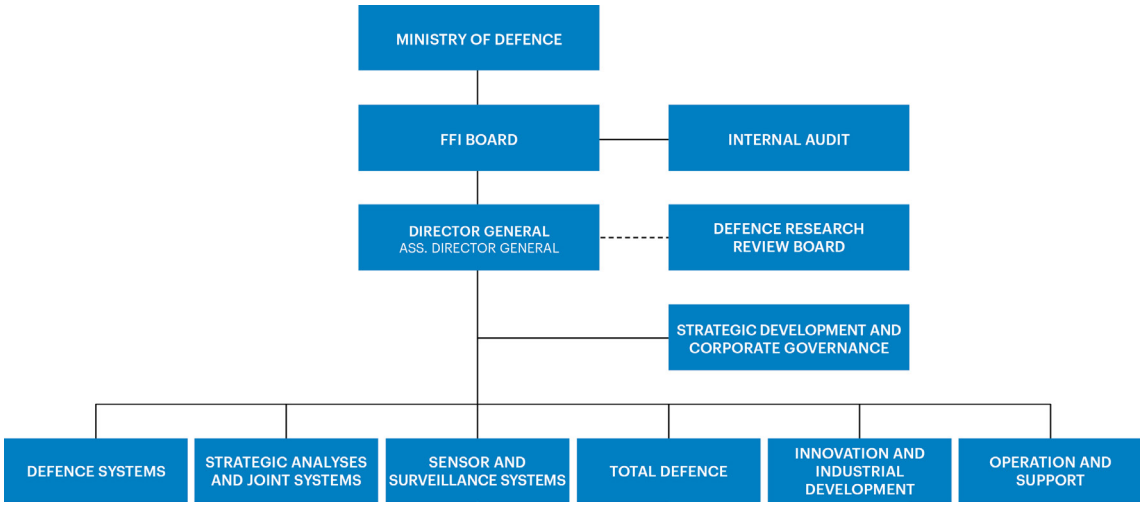

Forsvarets forskningsinstitutt (FFI)
Postboks 25
2027 Kjeller

Besøksadresse:
Kjeller: Instituttveien 20, Kjeller
Horten: Nedre vei 16, Karljohansvern, Horten

Telefon: 91 50 30 03
E-post: post@ffi.no
ffi.no

Norwegian Defence Research Establishment (FFI)
PO box 25
NO-2027 Kjeller
NORWAY

Visitor address:
Kjeller: Instituttveien 20, Kjeller
Horten: Nedre vei 16, Karljohansvern, Horten

Telephone: +47 91 50 30 03
E-mail: post@ffi.no
ffi.no/en